

Time Resolved Spectroscopy of Some Aromatic *N*-Oxide Triplets, Radical Anions, and Related Radicals

Xiaofeng Shi and Matthew S. Platz*

Department of Chemistry, The Ohio State University, 100 West 18th Avenue, Columbus, Ohio 43210

Received: December 4, 2003; In Final Form: March 9, 2004

Laser flash photolysis (LFP) and time-resolved infrared spectroscopy (TRIR) techniques and density function theory (DFT) calculations were used to investigate the electron-transfer chemistry of the triplet excited states of isoquinoline *N*-oxide (**1**), benzocinnoline *N*-oxide (**2**), and 4-nitroquinoline *N*-oxide (**3**). It was found that neither triplet **1** nor triplet **2** undergoes electron-transfer reactions with typical donors. Rather, they undergo net hydrogen atom transfer (proton-coupled electron transfer) with hydroquinone. Triplet 4-nitroquinoline *N*-oxide readily undergoes electron-transfer reactions as previously reported, to form the analogous radical anion and hydroxyl radical. The structures of these species were identified by LFP and TRIR techniques with the aid of DFT calculations. The oxygen atom on the *N*-oxide group was found to be the protonation site of the radical anion of **3**.

I. Introduction

Tirapazamine is an aromatic *N*-oxide used in the treatment of hypoxic tumors.¹ It is generally accepted that this drug is enzymatically activated to form a radical anion that is protonated to form a neutral radical.¹ Daniels et al.² have postulated that the neutral radical fragments to form hydroxyl radical, which subsequently damages cellular DNA. In this way, the oxygen atom of an aromatic *N*-oxide is effectively converted to a hydroxyl radical (Scheme 1).

We have reported that the excited singlet state of tirapazamine will undergo electron-transfer reactions.³ These processes are too rapid to study by nanosecond spectroscopy. Electron-transfer reactions of triplet tirapazamine (T_1) are not easily studied because of the low quantum yield of intersystem crossing in the S_1 state. That motivated this study of the photochemistry of simpler aromatic *N*-oxides to learn if their triplet states will undergo electron-transfer reactions that ultimately release hydroxyl radical. Herein, we are pleased to report our results.

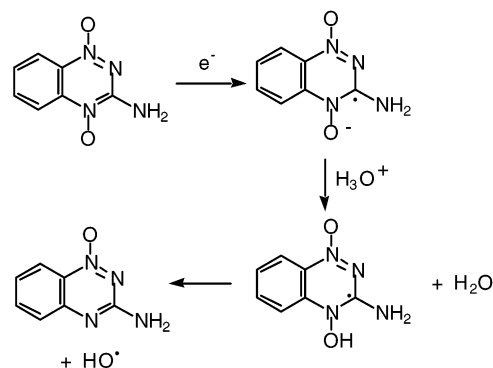
II. Experimental Section

Materials. Isoquinoline-*N*-oxide (**1**) and 4-nitroquinoline *N*-oxide (**3**) were purchased from Aldrich. Benzocinnoline *N*-oxide (**2**) was purchased from Acros. 4-Nitroquinoline (**4**) was prepared as described in the literature.⁴ 4-Hydroxyaminoquinoline *N*-oxide (**6**) was purchased from TCI. All of these chemicals were used as received. Solvents (acetonitrile, dichloromethane, and benzene) were distilled over calcium hydride before use.

Time-Resolved Infrared Spectroscopy. Time-resolved infrared spectroscopy (TRIR) experiments were performed and analyzed using the spectrometer previously described in the literature.⁵ Each sample solution was prepared with an optical density of 0.6–1.0 with a 0.5 mm path length. A total volume of 20–30 mL of sample was circulated between two barium fluoride or calcium fluoride salt plates. The sample was excited with a Nd:YAG laser of 355 nm wavelength at 97 Hz repetition rate with 0.5–0.7 mJ/pulse.

* Corresponding author. Phone: 614-292-0401. Fax: 614-292-5151. E-mail: platz.1@osu.edu.

SCHEME 1



Laser Flash Photolysis. Laser flash photolysis (LFP) experiments were also performed on the instrument described previously.⁶ Samples were excited with a Spectra Physics LAB-150–10 (~5 ns) water-cooled laser at the third harmonic frequency (355 nm) with a power of ~0.045 J/pulse.

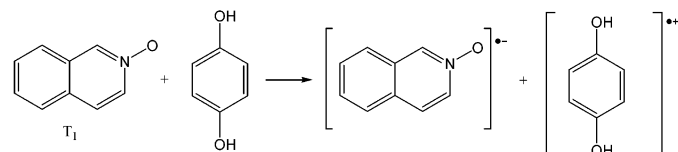
High-Pressure Liquid Chromatography. HPLC analyses were performed on a Beckman Coulter liquid chromatography system equipped with System Gold 168 diode array detector and controlled using an IBM computer and the 32 Karat 5.0 software package. Separations were achieved on a reverse phase C18 250 mm × 4.6 mm (5 μm) column preceded by a guard column. A mixture of HPLC grade water and methanol (2:3, v:v) was used as eluent at a flow rate of 0.75 mL/min. The identity of the products was established by comparison of their retention times and absorption spectra with those of authentic samples.

The concentration of the samples analyzed by HPLC was the same as that used in the LFP studies. The solutions contained in pyrex cuvettes were degassed by argon and irradiated with 350–365 nm light (Ray-O-Net reactor) for 8 h while stirred.

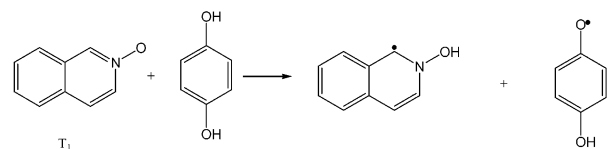
Computational Methods. All calculations were performed using the Gaussian 98 suite of programs⁷ at the Ohio Supercomputer Center (OSC). Geometries were optimized at the unrestricted B3LYP/6-31G* level of theory with single point

Isoquinoline *N*-oxide:

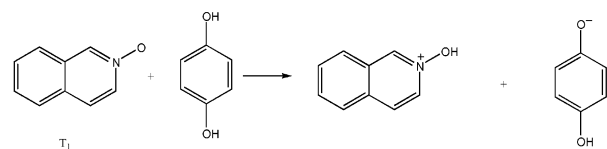
1) Electron transfer with hydroquinone

Gas phase: $\Delta H = 118.5$ kcal/molAcetonitrile: $\Delta H = 32.4$ kcal/mol

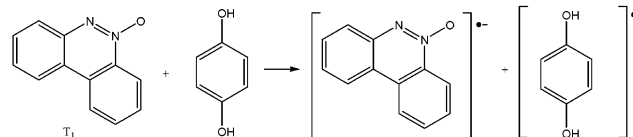
2) Hydrogen atom transfer

Gas phase: $\Delta H = -1.0$ kcal/molAcetonitrile: $\Delta H = -1.6$ kcal/mol

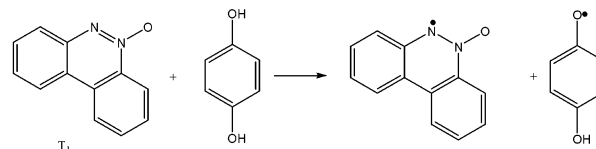
3) Proton transfer reaction

Gas phase: $\Delta H = 78.8$ kcal/molAcetonitrile: $\Delta H = 16.0$ kcal/molBenzocinnoline *N*-oxide:

1) Electron transfer with hydroquinone

Gas phase: $\Delta H = 172.8$ kcal/molAcetonitrile: $\Delta H = 25.3$ kcal/mol

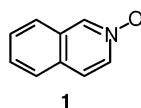
2) Hydrogen atom transfer

Gas phase: $\Delta H = -6.2$ kcal/molAcetonitrile: $\Delta H = -4.3$ kcal/mol**Figure 1.** Calculated reaction enthalpies of different reaction pathways of $^3\mathbf{1}^*$ and $^3\mathbf{2}^*$ with hydroquinone.

energies obtained at the B3LYP/6-31+G**//B3LYP/6-31G* level of theory. Vibrational frequency analyses at the B3LYP/6-31G* level were utilized to verify the energetic minima from the stationary points. The zero-point vibrational energy correction, scaled by a factor of 0.9804, and infrared spectra, scaled by a factor of 0.9613, were also obtained from the frequency analysis. Solution structures and energies were computed using the polarizable continuum model (PCM)⁸ provided by Gaussian 98. The electronic spectra were computed using the time-dependent DFT theory of Gaussian 98 at the B3LYP/6-31G* level, and 10 transitions were included.

III. Results and Discussion

III.1. Isoquinoline *N*-Oxide. LFP (355 nm) of isoquinoline-*N*-oxide (**1**) produces the previously reported transient spectrum of $^3\mathbf{1}^*$ in benzene, dichloromethane, and water at ambient temperature.⁹



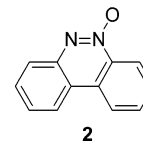
$^3\mathbf{1}^*$ reacts rapidly with oxygen, as expected, but reacts too slowly with typical electron (KSCN, NaI, NaN₃, 1,3,5-trimethylbenzene, DABCO, indole, and silylated guanosine), proton (benzoic acid), and hydrogen atom (tris(trimethylsilyl)silane) donors to allow measurement of those bimolecular quenching rate constants. The one exception to this pattern is hydroquinone, which undergoes a hydrogen atom transfer reaction (proton-coupled-electron transfer) with $^3\mathbf{1}^*$.¹⁰ A plot of the triplet decay

rate constant vs the concentration of hydroquinone was linear. The slope ($7.0 \times 10^6 \text{ M}^{-1} \text{ s}^{-1}$) is the bimolecular rate constant of $^3\mathbf{1}^*$ with hydroquinone.

The reactivity pattern of $^3\mathbf{1}^*$ was analyzed with the aid of DFT calculations. It was found that only a hydrogen atom transfer is a thermodynamically favorable process in both the gas phase and acetonitrile. Simple electron and proton transfer are both endothermic processes (Figure 1).

The photochemistry of **1** was also studied by time-resolved infrared spectroscopy. Unfortunately, we did not detect IR-active transients formed by LFP of **1** in dichloromethane. We suspect that the quantum yield of triplet formation is low due to ring-closure reactions in the singlet excited state, $^1\mathbf{1}^*$.

III.2. Benzocinnoline *N*-Oxide. LFP (355 nm) of benzocinnoline-*N*-oxide (**2**) in deoxygenated methanol at ambient temperature produces the transient spectrum of Figure 2.



The lifetime of the carrier of the transient spectrum is about $7 \mu\text{s}$ in deoxygenated methanol at ambient temperature. The transient spectrum is attributed to $^3\mathbf{2}^*$ because the carrier of the spectrum reacts rapidly with oxygen. The assignment of the transient spectrum to $^3\mathbf{2}^*$ is also based on the similarity of its reactivity pattern relative to that of $^3\mathbf{1}^*$. The triplet state of **2** reacts very sluggishly with electron, proton, and hydrogen atom donors. As with $^3\mathbf{1}^*$, the triplet state of **2** reacts only with hydroquinone among the quenchers studied. DFT calculations

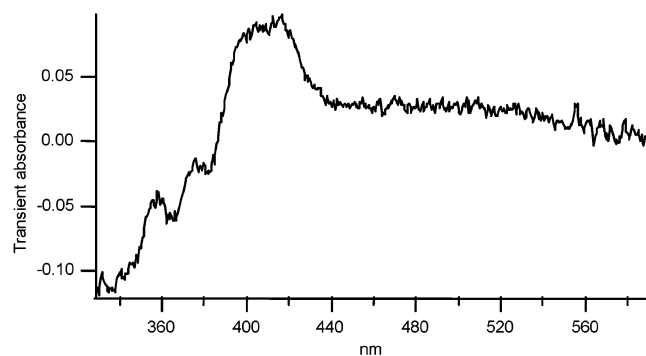


Figure 2. Transient spectrum produced by LFP (355 nm) of 0.1 mM benzocinnoline *N*-oxide in methanol. The spectrum was recorded 5 ns after the laser pulse over a 30 ns time window.

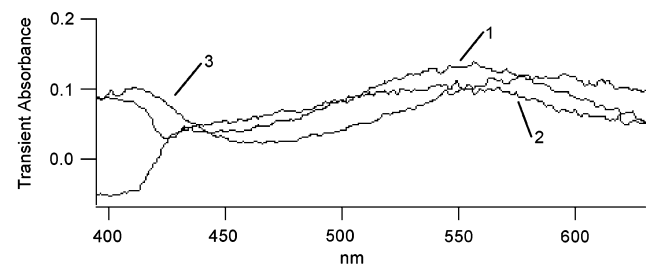
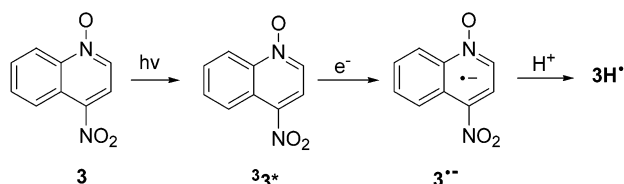


Figure 3. The transient spectra of $^3\mathbf{3}$ (0.35 mM) produced upon LFP (355 nm). The spectrum was recorded immediately after the laser pulse over a 45 ns time window. Solvent: 1, CH_2Cl_2 ; 2, benzene; 3, water.

of the reaction enthalpies of $^3\mathbf{2}^*$ with hydroquinone were also performed and predict that hydroquinone cannot undergo electron-transfer reaction with $^3\mathbf{2}^*$ while hydrogen atom transfer is energetically allowed (Figure 1).

III.3. 4-Nitroquinoline *N*-Oxide. Kasama et al.¹¹ and Seki and co-workers¹² have reported that photolysis of 4-nitroquinoline *N*-oxide $\mathbf{3}$ leads efficiently to its triplet state ($\lambda_{\text{max}} = 410$,



590 nm). They report further that $^3\mathbf{1}^*$ readily accepts electrons from donors such as guanosine and tryptophan in buffer solution to form a radical anion ($\mathbf{^3\mathbf{3}^{\bullet-}}$) which can be protonated to form a neutral hydro radical $\mathbf{^3\mathbf{H}^\bullet}$ ($\lambda_{\text{max}} = 460$ nm).^{11,12}

The nitro group has the desirable properties of enhancing the triplet state yield and the ease of its reduction. Both factors make $\mathbf{3}$ a promising photochemical source of hydroxyl radical by the Daniels, Gates, and Greenburg mechanism.²

Laser Flash Photolysis Studies. LFP (355 nm) of $\mathbf{3}$ in deoxygenated solvents produces the transient spectra of Figure 3. The transient spectra are in good agreement with previous reports and are attributed to $^3\mathbf{3}^*$. The transient spectrum of $^3\mathbf{3}^*$ is also in good agreement with time-dependent density functional theoretical (TD-DFT) calculations (Figure 4).

The TD-DFT predicted transient spectrum of radical anion $\mathbf{^3\mathbf{3}^{\bullet-}}$ is also shown in Figure 4 and its main band is predicted to be near that of $^3\mathbf{3}^*$.

LFP of $\mathbf{3}$ (335 nm) in acetonitrile containing 8 mM diazabicyclooctane (DABCO) produces the transient spectrum of Figure 5. The large band at 508 nm is attributed to radical anion $\mathbf{^3\mathbf{3}^{\bullet-}}$, which is consistent with the predictions of TD-DFT calculations.

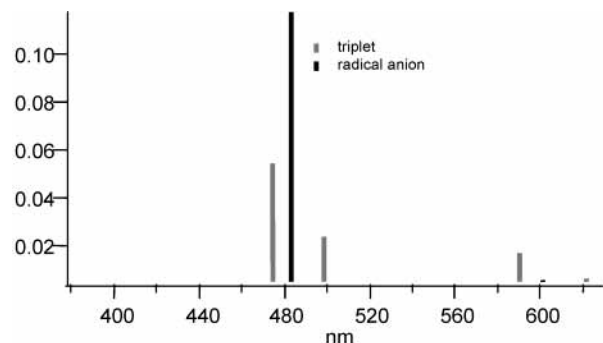
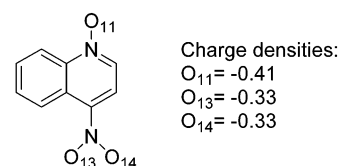


Figure 4. The calculated UV-vis spectra of $^3\mathbf{3}^*$ and $\mathbf{^3\mathbf{3}^{\bullet-}}$ in the gas phase.

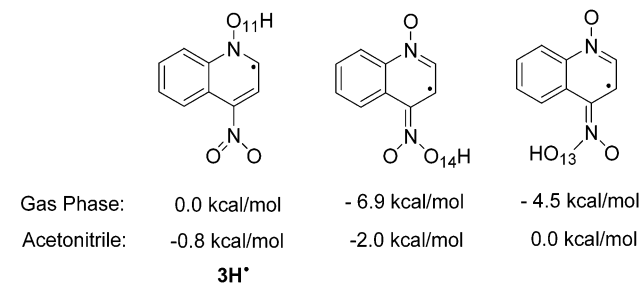
The shoulder in the transient spectrum of Figure 5 at 480 nm is assigned to the DABCO radical cation, which is known to absorb in this region.¹³

The transient spectrum obtained by LFP of $\mathbf{3}$ in the presence of 8 mM DABCO in acetonitrile containing 20% water (v/v) is given in Figure 6. The spectrum recorded immediately after the laser pulse is that of the radical ions. The spectrum recorded 5 μs after the laser pulse is that of a different species with a broad absorption around 450 nm. The carrier of this absorption is attributed to the neutral hydroradical $\mathbf{^3\mathbf{H}^\bullet}$ formed by protonation of radical anion $\mathbf{^3\mathbf{3}^{\bullet-}}$ by water, in excellent agreement with pulse radiolysis studies.¹²

What is the structure of the hydroradical? A natural population analysis of radical anion $\mathbf{^3\mathbf{3}^{\bullet-}}$ gives the charge densities listed below.



As the oxygen atom of the *N*-O bears the most negative charge, one might expect that O_{11} of $\mathbf{^3\mathbf{3}^{\bullet-}}$ will be the kinetic site of protonation. We have calculated the relative energies of each of the hydroradicals produced by protonation of O_{11} , O_{13} , and O_{14} in the gas phase and in acetonitrile. In acetonitrile, where



most LFP and TRIR experiments were performed, the hydroradical obtained by protonation of O_{14} has the lowest energy by 2.0 kcal/mol. Given the normal error of those calculations, we cannot conclusively determine the structure of $\mathbf{^3\mathbf{H}^\bullet}$ solely by comparing the computed relative energies. However, the predicted UV-vis spectrum of the hydroradicals (Figure 7) in acetonitrile suggests that the transient spectrum observed (strong absorption over 400 nm) is the hydroradical protonated at the *N*-oxide oxygen (O_{11}). This will be confirmed by time-resolved infrared spectroscopy.

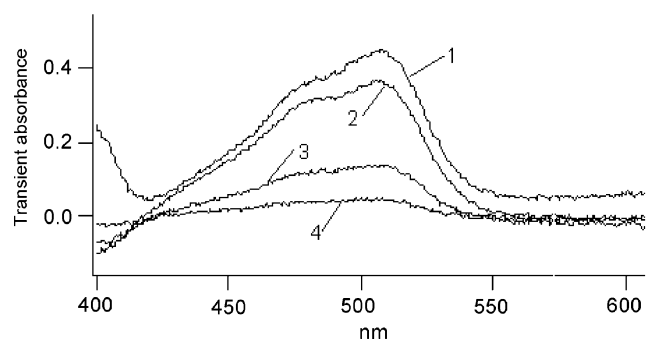


Figure 5. The transient spectra produced upon LFP (355 nm) of 0.3 mM **3** and 8 mM DABCO in acetonitrile: 1, immediately after laser pulse; 2, 500 ns after laser pulse; 3, 3 μ s after laser pulse; 4, 10 μ s after laser pulse.

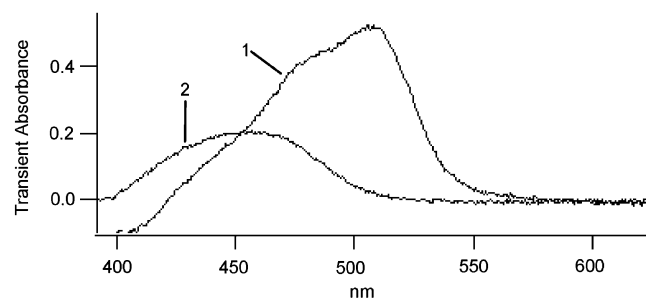


Figure 6. The transient spectra produced upon LFP (355 nm) of 0.3 mM **3** and 8 mM DABCO: 1, immediately after laser, in acetonitrile; 2, 5 μ s after laser pulse, in 80% acetonitrile, 20% water (v:v).

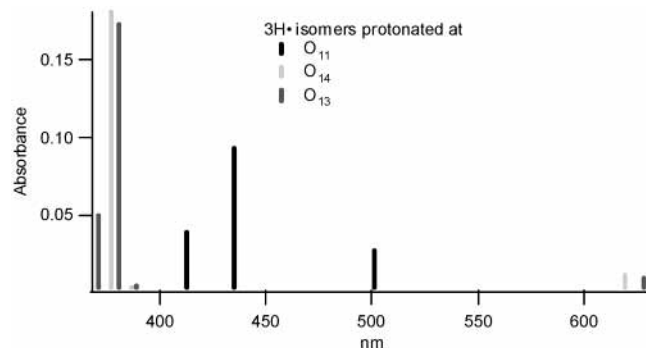


Figure 7. The calculated UV-vis spectra of different isomers of **3H•** in acetonitrile.

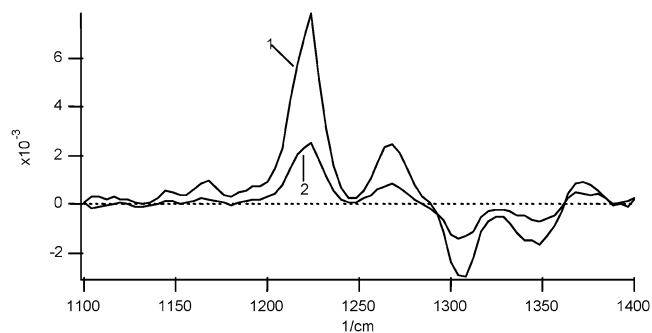


Figure 8. The transient IR spectra produced upon LFP (355 nm) of 3 mM **3** in acetonitrile (1100–1300 cm^{-1}) and CH_2Cl_2 (1300–1400 cm^{-1}). Window: 1, 0–1 μ s; 2, 3–4 μ s.

Time-Resolved Infrared (TRIR) Spectroscopy. LFP (355 nm) of **3** in deoxygenated acetonitrile produces the TRIR spectrum of Figure 8. Two transient bands are observed at 1220 and 1270 cm^{-1} with lifetimes of 1.3 μ s. Vibrational bands of the precursor are bleached at 1304 and 1350 cm^{-1} (also at 1520

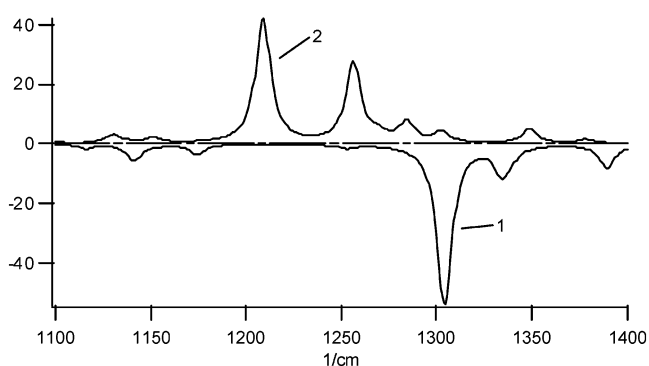


Figure 9. The calculated IR spectra of (1) **3** and (2) **33*** in acetonitrile.

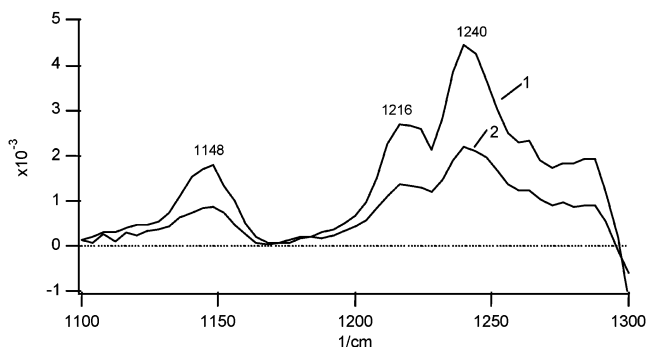


Figure 10. The transient IR spectra produced upon LFP (355 nm) of 3 mM **3** and 8 mM DABCO in acetonitrile. Window: 1, 0–1 μ s; 2, 3–4 μ s.

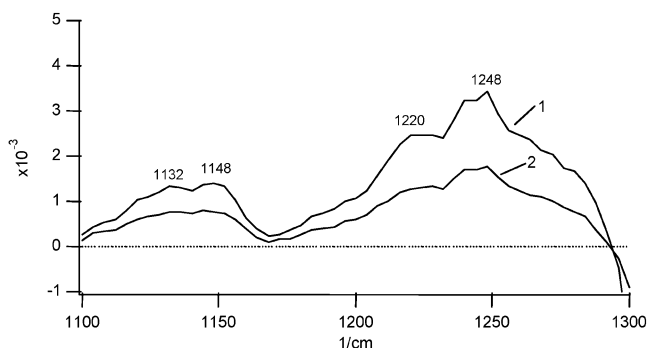


Figure 11. The transient IR spectra produced upon LFP (355 nm) of 3 mM **3**, 8 mM DABCO, and saturated NH_4Cl in acetonitrile. Window: 1, 0–2 μ s; 2, 6–8 μ s.

and 1566 cm^{-1} ; Supporting Information), which fully recover with a time constant of 1.5 μ s (1304 cm^{-1}) and 1.3 μ s (1520 cm^{-1}). This leads us to assign the phototransients absorbing at 1220 and 1270 cm^{-1} to the triplet state of **3** (**33***). These assignments are consistent with DFT calculations (Figure 9), which predict that **33*** will have prominent vibrations at 1230 and 1280 cm^{-1} after scaling by a factor of 0.9613.

LFP of **3** and 8 mM DABCO in deoxygenated acetonitrile produces the transient spectrum of Figure 10. The spectrum exhibits a biexponential decay ($\tau = 0.63$ and 3.5 μ s, Figure 14), which leads us to assign the transient spectra to a mixture of **33*** and its long-lived radical anion **3•-**.

LFP of a mixture of **3**, 8 mM DABCO, and saturated ammonium chloride in deoxygenated acetonitrile produces the transient spectra of Figure 11. The transients exhibit biexponential decay ($\tau = 0.9$ and 14 μ s), which leads us to assign the spectra to a mixture of radical anion **3•-** and hydroradical **3H•**. DFT calculations predict that **3•-** and **3H•** will have similar

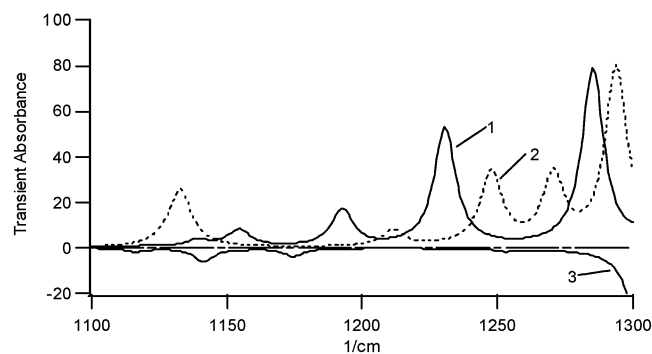


Figure 12. The calculated IR spectra of **3** (down) and **3**^{•-} (up) in the acetonitrile.

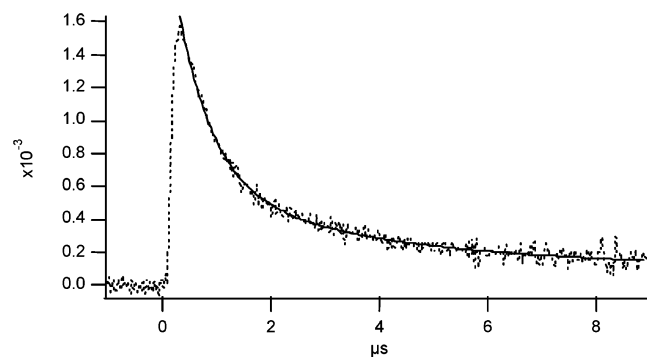


Figure 13. The decay of the 1240 cm^{-1} transient produced upon LFP (355 nm) of 3 mM **3** and 8 mM DABCO in acetonitrile. Double exponential decay: $\tau = 0.63$ and $3.5\ \mu\text{s}$, respectively.

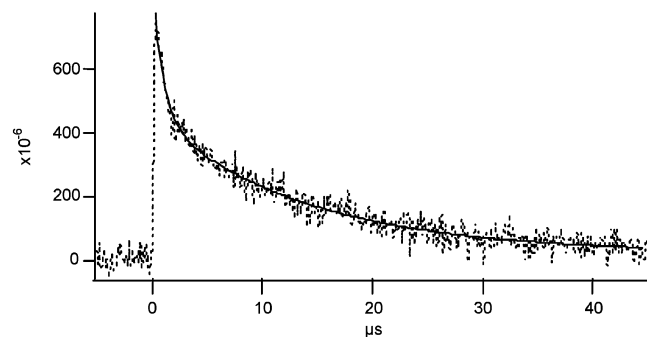


Figure 14. The decay of the 1240 cm^{-1} transient produced upon LFP (355 nm) of 3 mM **3**, 8 mM DABCO, and saturated NH_4Cl in acetonitrile. Double exponential decay: $\tau = 0.9$ and $14\ \mu\text{s}$, respectively.

vibrational spectra in this region (Figure 12). The two species of interest have distinctly different lifetimes, however (Figures 13 and 14).

DFT calculations were performed to predict the IR spectra of the three possible neutral hydro radicals that can be formed upon protonation of the three different oxygen atoms of the radical anion of **3**^{•-}. The region between 1100 and 1300 cm^{-1} is not decisive in distinguishing among the possible isomers. All the possible hydroradicals **3H**[•] are predicted by theory to have vibrational bands due to the stretching of the ring double bonds in the region between 1400 and 1470 cm^{-1} . However, only the hydroradical obtained by protonation of O_{11} has a strong absorption at 1420 cm^{-1} caused by the N–O–H in-plane bending (Figure 15), while neither the other two hydroradical isomers obtained by protonation of O_{13} and O_{14} nor the radical anion is predicted to have a prominent IR band in this region. As shown in Figure 16, LFP of a mixture of **3**, 8 mM DABCO, and saturated ammonium chloride in acetonitrile- d_3 leads to transient absorption at 1410 and 1450 cm^{-1} with $\tau = 9\ \mu\text{s}$

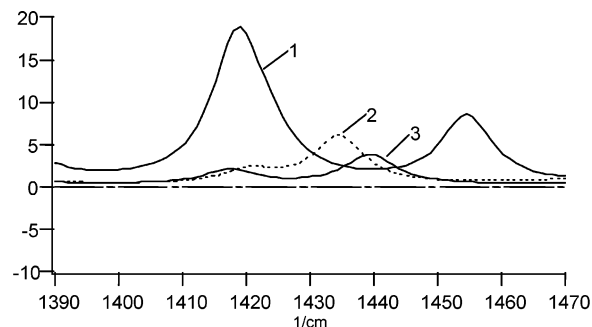


Figure 15. The calculated IR spectra of **3H**[•] protonated at (1) O_{11} , (2) O_{14} , and (3) O_{13} in acetonitrile.

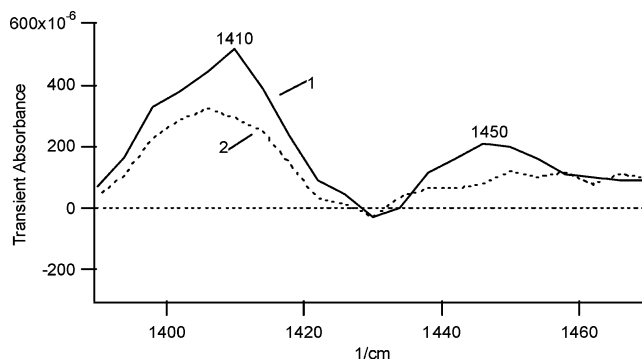


Figure 16. The transient IR spectra produced upon LFP (355 nm) of 3 mM **3**, 8 mM DABCO, and saturated NH_4Cl in acetonitrile- d_3 upon 355 nm LFP. Window: 1, 0–2 μs ; 2, 6–8 μs .

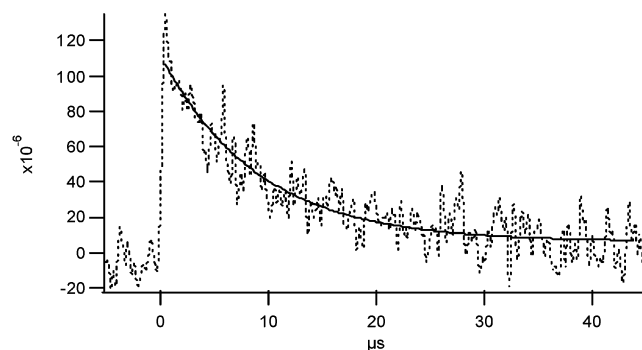


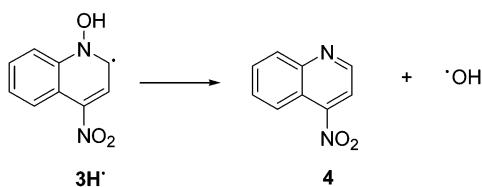
Figure 17. The decay of the 1410 cm^{-1} absorbing transient produced upon LFP (355 nm) of 3 mM **3**, 8 mM DABCO, and saturated NH_4Cl in acetonitrile- d_3 . Single-exponential decay: $\tau = 9\ \mu\text{s}$.

(Figure 17). This is in good agreement with theory, which predicts absorptions at 1420 (O–H bending) and 1455 cm^{-1} (ring double bond stretching) (Figure 15). The other hydroradical (protonated at O_{14} or O_{13}) isomers are predicted to have distinct absorptions between 850 and 950 cm^{-1} , but no absorptions were observed in this region.

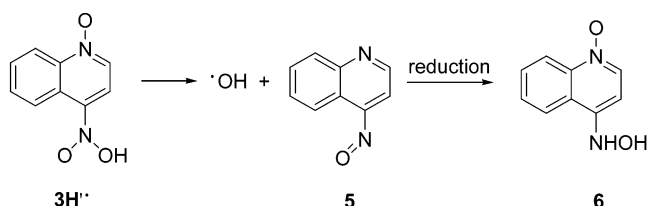
Since both TRIR and LFP transient spectroscopy suggest that the protonation proceeds at the O_{11} position of the *N*-oxide, it seems likely that this hydroradical will fragment to form hydroxyl radical and 4-nitroquinoline, **4**. HPLC analysis indicates that the major product formed on photolysis of 4-nitroquinoline *N*-oxide in acetonitrile is 4-nitroquinoline.¹⁴ However, the presence of DABCO and ammonium chloride quenches the formation of 4-nitroquinoline, instead of enhancing the yield of **4** through the dehydroxylation mechanism. Thus, electron-transfer conditions do not lead to a hydroradical that fragments to form hydroxyl radical and 4-nitroquinoline.

DFT calculations explain why the fragmentation of the hydroxyl radical formed by the protonation of O_{11} is not

favorable in acetonitrile (ΔH_f from $3\text{H}\bullet$ to **4** is computed to be 11.3 kcal/mol). This also explains the relatively long lifetime of this hydradical.



DFT calculations indicate that protonation of O_{14} will also form a radical, $3\text{H}'\bullet$, with a lifetime sufficiently long to allow its detection (ΔH_f from $3\text{H}'\bullet$ to **5** is predicted to be 34.3 kcal/mol). However, we did not observe the radical ($3\text{H}'\bullet$) in LFP and TRIR experiments.



We conclude that the fragmentation proposed by Seki et al.¹¹ is not thermodynamically reasonable in solution. In support of this view, we note that 4-hydroxyaminoquinoline *N*-oxide, **6**, the product of reduction of **5**, is not observed by the HPLC analysis of the mixture of photolysis products of 4-nitroquinoline *N*-oxide in the presence of DABCO and ammonium chloride.

IV. Conclusions

The triplet states of isoquinoline *N*-oxide and benzocinnoline *N*-oxide react sluggishly with electron (KSCN, NaI, NaN_3 , 1,3,5-trimethylbenzene, DABCO, indole, and silylated guanosine), proton (benzoic acid), and hydrogen atom (tris(trimethylsilyl)silane) donors. These triplets will react with hydroquinone by hydrogen atom transfer (proton-coupled electron transfer). Triplet 4-nitroquinoline *N*-oxide reacts readily with electron donors to form the radical anions as previously reported. The radical anion is protonated on the oxygen atom of the *N*-oxide group to form a neutral radical. The triplet state, radical anion, and neutral hydradical derived from 4-nitroquinoline *N*-oxide were detected by TRIR spectroscopy, and the spectra were interpreted with density functional theory calculations. The three

N-oxides of this study are not expected to serve as photochemical sources of hydroxyl radical.

Acknowledgment. Support of this work by the National Science Foundation-EMSI-CHE0089147 at OSU and the Ohio Supercomputer Center is gratefully acknowledged.

Supporting Information Available: TRIR spectra of 3 mM **3** in dichloromethane scanned between 1600 and 1500 cm^{-1} with a recovery kinetic trace at 1520 cm^{-1} , geometries, energies, S^2 values, thermal corrections, frequencies, IR intensities, energetic gaps of electronic states, and oscillation factors in the gas phase and in acetonitrile. This material is available free of charge via the Internet at <http://pubs.acs.org>.

References and Notes

- (1) (a) Brown, J. M. *Br. J. Cancer* **1993**, *67*, 1163. (b) Brown, J. M.; Siim, B. G. *Seminars Rad. Oncol.* **1996**, *6*, 22. (c) Brown, J. M.; Wang, L.-H. *Anti-Cancer Drug Design* **1998**, *13*, 529. (d) Brown, J. M. *Cancer Res.* **1999**, *59*, 5863.
- (2) (a) Daniels, J. S.; Gates, K. S. *J. Am. Chem. Soc.* **1996**, *118*, 3380. (b) Daniels, J. S.; Gates, K. S.; Tronche, C.; Greenberg, M. M. *Chem. Res. Toxicol.* **1998**, *11*, 1254.
- (3) Poole, J. S.; Hadad, C. M.; Platz, M. S.; Fredin, Z. P.; Pickard, L.; Guerrero, E. L.; Kessler, M.; Chowdhury, G.; Kotandeniya, D.; Gates, K. S. *Photochem. Photobiol.* **2002**, *75*, 339.
- (4) Kaneko, C.; Yamamoto, A.; Gomi, M. *Heterocycles* **1979**, *12*, 227.
- (5) Martin, C. B.; Tsao, M. -L.; Hadad, C. M.; Platz, M. S. *J. Am. Chem. Soc.* **2002**, *124*, 7226.
- (6) Martin, C. B.; Shi, X.; Tsao, M.-L.; Karweik, D.; Brooke, J.; Hadad, C. M.; Platz, M. S. *J. Phys. Chem. B* **2002**, *106*, 10263.
- (7) Frisch, M. J.; Trucks, G. W.; Schlegel, H. B.; Scuseria, G. E.; Robb, M. A.; Cheeseman, J. R.; Zakrzewski, V. G.; Montgomery, J. A., Jr.; Stratmann, R. E.; Burant, J. C.; Dapprich, S.; Millam, J. M.; Daniels, A. D.; Kudin, K. N.; Strain, M. C.; Farkas, O.; Tomasi, J.; Barone, V.; Cossi, M.; Cammi, R.; Mennucci, B.; Pomelli, C.; Adamo, C.; Clifford, S.; Ochterski, J.; Petersson, G. A.; Ayala, P. Y.; Cui, Q.; Morokuma, K.; Malick, D. K.; Rabuck, A. D.; Raghavachari, K.; Foresman, J. B.; Cioslowski, J.; Ortiz, J. V.; Baboul, A. G.; Stefanov, J. V.; Liu, G.; Liashenko, A.; Piskorz, P.; Komaromi, I.; Gomperts, R.; Martin, R. L.; Fox, D. J.; Keith, T.; Al-Laham, M. A.; Peng, C. Y.; Nanayakkara, A.; Gonzalez, C.; Challacombe, M.; Gill, P. M. W.; Johnson, B.; Chen, W.; Wong, M. W.; Andres, J. L.; Gonzalez, C.; Head-Gordon, M.; Replogle, E. S.; Pople, J. A. *Gaussian 98*, revision A.7; Gaussian, Inc.: Pittsburgh, PA, 1998.
- (8) Tomasi, J.; Persico, M. *Chem. Rev.* **1994**, *94*, 2027.
- (9) Ono, I.; Hata, N. *Bull. Chem. Soc. Jpn.* **1973**, *46*, 3658.
- (10) Binstead, R. A.; McGuire, M. E.; Dvletoglou, A.; Seok, W. K.; Roecker, L. E.; Meyer, T. J. *J. Am. Chem. Soc.* **1992**, *114*, 173.
- (11) Kasama, K.; Takematsu, A.; Yamamoto, S.; Arai, S. *J. Phys. Chem.* **1984**, *88*, 4918.
- (12) Seki, H.; Takematsu, A.; Arai, S. *J. Phys. Chem.* **1987**, *91*, 176.
- (13) Shida, T. *Electronic Absorption Spectra of Radical Ions*; Elsevier: Amsterdam, 1988.
- (14) The mechanism by which this product is formed is not known. DFT calculations predict that direct fragmentation of triplet 4-nitroquinoline *N*-oxide to 4-nitroquinoline and oxene is endothermic by 29.5 kcal/mol in acetonitrile.